TEXTILE-REINFORCED RAMMED EARTH: EXPERIMENTAL CHARACTERISATION OF FLEXURAL STRENGTH AND THOUGHNESS

Ernest Bernat[a*], Lluís Gil[a] and Christian Escrig[a]

[a] *Department of Strength of Materials and Engineering Structures*

Technical University of Catalonia. Colom 11. 08222 Terrassa, Spain

ABSTRACT

Rammed earth is a building material that has gained attention because of its sustainable advantages. However, its negligible tensile strength and its lack of strain energy dissipation may compromise some structures. This work proposes the use of textile grids as reinforcement systems for rammed earth. An adapted methodology to assess the effect of embedding fibre grids is presented. The maximum bending moment and the flexural toughness was determined for 26 specimens by using different types of grids. It was determined that using a flexible fibre grid with large spacing between fibre tows was the most efficient option, as it duplicated the flexural strength and increased the flexural toughness by a factor of sixty.

KEYWORDS

Textile reinforcement, Rammed earth, Strength, Flexural Toughness, Experimental

[*] Corresponding author:

Tel.: +34 937398728; fax: 937398994

e-mail address: ernest.bernat@upc.edu

1. Introduction

Earthen building technologies (such as earth block masonry, adobe, rammed earth, or cob, among others, see the work by Miccoli et al. [1]) have been used worldwide for thousands of years because of the simplicity of the construction procedure, the availability of materials (earth) and the properties of the resulting structures. However, the use of these traditional construction techniques became sparse with the development of concrete and steel materials, which allowed for the production of buildings with lower workforce requirements. As a result, in comparison with other construction technologies, research on earthen construction has received significantly less attention.

However, earthen architecture is increasingly gaining supporters due to the sustainable advantages of using earth as a building material. The most important benefits include the use of a local material obtained in situ, thereby eliminating transportation costs and associated CO_2 emissions; the complete recyclability of the building structure, the thermal inertia; and the architectural plasticity. The survey carried out by Niroumand et al. [2] certified that there is an increasing interest in earthen construction, but that this interest is limited by some drawbacks. These drawbacks include the most important limitation that earthen construction lacks a scientific basis and the corresponding standards to use it with the same confidence levels as other current construction materials.

Recent research attempts to fill this gap in knowledge. The research on earthen construction has covered a wide range of issues, but most of the investigations have focused on two main aspects, namely, the thermal efficiency and the requirements of the component materials (clay, silt, sand, gravel, water and additives) to reach an optimum solution in terms of strength and durability. In the context of thermal efficiency, it is worth highlighting the work by Heathcote [3], who pointed out that earth buildings have poorer thermal isolation than clay brick buildings. However, the larger thermal inertia of earth softens the temperature changes, which translates into a comfortable sensation for people.

The influence of the moisture on the earth mixture is important with respect to the requirements of the component materials. Schroeder [4] analysed the drying process of earthen elements and concluded that there is a relationship between the initial moisture, the drying process and the final strength of rammed earth walls. Additionally, research was carried out by Ciancio et al. [5], Jiménez et al. [6] and Da Rocha et al. [7] on determining the dosage and specifications of the solid component materials (clay, silt, sand, gravel) and the expected properties of the mixed material before it was used to achieve the maximum density, compressive strength or erosion strength. A few studies have focused on the durability of earthen constructions and potential alternatives to enhance the lifespan of earthen constructions. Maldonado [8] focused on analysing the influence of superficial treatments and using consolidating additives to improve the strength of rammed earth walls against water erosion. However, Ciancio et al. [5] noted that the variability of the earthen properties and their composition makes it impossible to specify general rules about the components. It is only possible to propose and analyse the minimum requirements of the final earthen elements.

Although knowledge about earthen construction has increased due to past research, there are still some technical issues that limit the practical use of earthen construction, including the almost negligible tensile strength and limited capacity to dissipate energy once the material is cracked. With respect to these issues, there have been a few proposals to overcome the tensile strength and energy dissipation limitations. These proposals can be divided in two groups, namely, proposals aimed to externally strengthen earthen structures and proposals aimed to provide a reinforcing system placed inside earthen material when casting the structure. In fact, some types of ancient earthen techniques (such as adobes and cobs) involve adding natural fibres to the earth mixture. However, this particular practice was more oriented to prevent shrinkage cracking than to provide effective tensile strength. Moreover, there is a paucity of research assessing of the energy dissipation capabilities of these particular buildings.

Reinforcing rammed earth walls allows the introduction of a new construction methodology to produce safe buildings in areas where it is difficult to procure Portland cement, wood or steel. Developing cheap fibre grids that are composed of available materials would be a sustainable evolution for this particular application if these reinforcing techniques prove to be efficient. Reinforced rammed earth walls would also open new construction possibilities in those territories where the environmental responsibility is a priority, but where there are strict requirements for structural safety. Developing and improving reinforced rammed earth would allow the production of environmental-friendly small and medium height low-cost buildings. Given these reasons, research on reinforcing and strengthening rammed earth has gained attention in recent years.

Blondet et al. [9] worked on both reinforcing and strengthening techniques and proposed using reeds embedded into earth walls to produce seismic-resistant earthen constructions and placing steel grids that are externally bonded with an inorganic plaster (mostly mud) to repair earthquake damaged walls. Liu et al. [10] proposed a strengthening system consisting of high performance fibres, which can be externally bonded to earth walls using adhesives. Furthermore, Tarque et al. [11] proposed a numerical model to simulate externally strengthened adobe walls in which the strengthening system was mechanically attached to the wall.

The procedure of using a high performance fibre grid embedded into an inorganic matrix to externally strengthen structures is commonly known as Textile Reinforced Mortar (TRM) or Fabric Reinforced Cementitious Matrix (FRCM). Several studies have focussed on the application of this strengthening technique on masonry and concrete elements. These involve different points of view, including experimental (see [12,13]), analytical (see [14]) and numerical simulations (see [15,16]).

The aim of this paper is to apply the knowledge that was generated through the study of the TRM in the recent years to propose a reinforcing system for rammed earth walls. This technical solution holds the potential to increase the dissipated energy in flexion based on which earth-quake resistant low cost buildings of reinforced rammed earth can be produced. This follows the proposals of Blondet et al. [9] and Barrionuevo [17].

A comprehensive experimental campaign focused on analysing the structural response of fibre grid reinforced rammed earth specimens is presented herein. Different types of fibre grids

were considered, and the influence of the reinforcement pattern was also analysed for a particular fibre grid. The tests focused on analysing the flexural toughness (which is an indirect measurement of the applied energy to break a specimen) of samples tested under three-point bending conditions. Thus, the Japanese Standard JSCE-SF4 [18] was taken into account as a reference, as in previous experimental studies (see [19]).

2. Methodology. Experimental campaign

The experimental campaign aimed to analyse the variation of the flexural strength and toughness of rammed earth specimens when fibre grids were embedded into them. Additionally, the influence of the fibre grid type on the mechanical response was also studied as a main property defining a reinforcing system.

2.1. Materials and Specimens

For the experimental campaign, 26 prisms of rammed earth were produced. These prisms were 350-mm long and had a cross section of 100 mm x 100 mm. Four of them were not reinforced, and the rest were reinforced with embedded fibre grids.

Clay, silt, sand and water were mixed; moulded; and pressed to produce rammed earth prisms. The manufacturing technology used here can be directly used to manufacture compressed earth blocks (CEB). However, the resulting CEB specimen represents a small portion of the rammed earth material.

A local company (*Sorres i graves Egara S.A.*) provided the earth components. The particle size distribution of the earth components mixed together (nomogram) is presented in Figure 1. This resulting distribution was analytically obtained from the particle size distribution of each component provided by the supplier and the dosage of each component (40.0% of clay/silt, 45% of sand with particles up to 2 mm and 15% of sand with particles up to 5 mm). It should be noted that the used mixture had a slightly higher portion of sand and less clay/silt than the general recommendations for rammed earth, as summarised by Jiménez et al. [6]. This may contribute to reducing the mechanical performance of the specimens, highlighting the effect of the reinforcing system. However, the tests on the unreinforced specimens (presented later in the paper) suggest that the specimens reached the expected flexural strength. This is in comparison with prior research, such as that of Ciancio et al. [5], who proposed a flexural strength of approximately 0.25MPa or slightly higher.

Suitable amount of water to be mixed with soil were experimentally determined by comparing the results of drop ball tests with different water contents. The drop ball test is a method that is used to assess the workability and binding capacity of soil mixtures that are to be used in earthen construction. It consists of dropping a ball that has a diameter of 2-3 cm from a height of 1.5 m and observing the consistency of the dropped ball. The ball should break in three parts, but not disintegrate nor remain as one piece. After determining the suitable amount of water to be added to the mixture, samples that had this water content were weighed both before and after drying them in an oven at 105˚C for 24hours. The weight difference expressed as a ratio over the dry weight was used as the moisture content, which was calculated as 12.6%.

The fibre grids that were used were composed of glass fibre, carbon fibre, steel cords, Poliparafenil-benzobisoxazole (PBO) fibres, and basalt fibres (Figure 2). It is worth mentioning that all of the textiles possessed a high grade of flexibility, which permitted a complete adaptation to different forms and shapes. The only exception to this was the steel cords grid. With regard to workability, the grids that had more space between tows/cords performed better than those that had a greater fibre density. This was because the earth penetrated into the textile more easily in the cases where the grid had a larger mesh cell. The mechanical and geometrical properties of the used fibre grids and the component fibres are summarised in Table 1. These values were provided by the suppliers of these materials and are commonly used for Textile Reinforce Mortar (TRM) applications.

The manufacturing process of the samples consisted of the following steps:

- The first step involved assembling the mould that had interior marks indicating the level where the fibre grids should be placed. The interior faces of the mould were made of pinewood and covered with a common plastic film to prevent the rammed earth from attach to the mould when pressed. The base of the mould was removable.
- In the second step, the mould was filled with layers of material, including earth and textile grids. For the cases without fibres, a single layer of 75 mm was filled up. For the cases with fibre grids embedded, first a layer of 20 mm of earth was set, and then, the reinforcement grid (measured 330 mm x 80 mm) was placed, and finally, the mould was filled with earth until it reached 75 mm.
- The next step entailed pressing the earth inside the mould with an electromechanical actuator for few seconds. The pressure was transmitted to the earth through a steel plate to uniformly distribute the 10.5 kN applied force. The result was a sample that had an approximate 50-mm height.
- Then, the mould was filled with an additional 75 mm of the earth mixture and was pressed again with a force of 10.5 kN.
- Finally, the specimen, which was kept on the mould base until it dried, was unmoulded.

The tested specimens are listed in Table 2, which summarizes the geometrical properties and reinforcing system of each sample. Figure 3 can be referred to for a better explanation. The manufacturing procedure was slightly modified for samples reinforced with two fibre grids. In the case of specimen 2G1 and 2G2, two glass fibre grids were placed together alternating the fibre tows to obtain half of the spacing between the fibre tows. In the case of specimen 2GL1 and 2GL2, two glass fibre grids were placed at different heights separated by 20 mm.

It should be noted that a specimen reinforced with the steel grid and a specimen reinforced with the PBO grid were damaged during the specimen manipulation after curing. The lower portion of the specimen detached (see Figure 4). Thus, the reinforcing grid became a weak surface in these cases. Additionally, this was observed for all of the specimens reinforced with steel in the form of a continuous horizontal crack. An additional specimen was produced with the steel fibre grid, but the damaged PBO specimen was not replaced. The damaged specimens are not considered in the rest of the paper.

2.2. Testing set up and sensors

Two weeks of drying at environmental indoor conditions assured that a final moisture content between 1% and 2% was reached, according with the experimental evidence. Following this, the specimens were tested in a three-point bending configuration.

As there are no specific test procedures to determine the flexural strength and toughness of fibre grid reinforced rammed earth specimens, the test setup followed the Standard JSCE-SF4 [18]. This code was initially developed to determine the flexural strength and toughness of fibre reinforced concrete. However, it has been successfully applied, with some modifications of the data analysis, to other materials, such as TRM strengthened masonry [19] or TRM shear strengthened concrete beams [14].

Thus, the specimens (350 mm long) were supported on two rods leaving a free span (*L*) of 300 mm. A third rod was fixed to the mobile part of an electromechanical press, and this was used to apply an imposed displacement at the middle of the top face of the sample. The displacement control assured capturing the post-peak response of the structure. This is crucial in assessing the flexural toughness of the specimen. The displacement was applied at a constant rate of 5 mm/min.

The applied force was read with a 50-kN load cell (10N precision) connected to the central mobile rod. The vertical displacement of the top face of the specimen at mid-span was read by the internal displacement sensor of the electromechanical press (0.01 mm precision). All data were simultaneously recorded at 5Hz. The test setup is shown in Figure 5.

3. Results

The results of the three-points bending tests are presented in this section. First, the calculation methodology is introduced. Then, the failure mode, the qualitative associated results and the observations during the tests are summarised; the flexural strength in terms of the maximum bending moment and the measured response are also presented. The results of the flexural toughness factor, which is the crucial comparison variable, are presented at the end of this section.

3.1. Data analysis

The flexural toughness was calculated by following the Standard JSCE-SF4 [18], but some modifications were introduced. Flexural toughness is defined as the area below the force-displacement curve (in linear scales), and it is a measure of the energy absorbed by the structural system to develop cracks and reach failure.

The methodology to calculate the flexural toughness of the specimens was adapted to the specifications and practical requirements of the tested material. This includes that a) all samples showed large displacements (up to *L/4*), b) there was a large dispersion of the ultimate deflection, c) for some reinforced cases the applied force after cracking descended to 0 N and then increased again because of the effect of the fibre grid, and d) the load-bearing capacity of all specimens was the most stable variable among the analysed ones.

Due to the large displacements, the threshold value of the maximum displacement for concrete (L/150), commonly considered for the calculation of the flexural toughness, was not suitable in this case. The assumption of this limit would have left most of the post-peak response (and even in a few cases the actual peak value) out of the analysis. In addition, the large scattering of the ultimate deflection prevented the consideration of this magnitude as a reasonable threshold value for the calculations.

In this paper, it was assumed that the specimen collapses when it cannot withstand any force. Hence, no further data were considered for the calculation of the flexural toughness, although the sample might have withstood higher loads if the test continued due to the tensile strength of the reinforcing grid. It may be observed that the percentage of the load-bearing capacity is a stable parameter and it is directly related to the applied energy. Therefore, the flexural toughness calculation used this variable for comparison.

Hence, after taking all of the mentioned distinctive features into account, it was decided to set a limit on the applied force as the ratio of the applied force to the load-bearing capacity of each specific test. The ratio used a threshold value of 10%, which allowed the majority of the post-cracking response was associated with a non-negligible flexural strength of the tested cases. This threshold value set the last data point to calculate the flexural toughness ($TEN_{F/10}$) of the unreinforced and reinforced rammed earth specimens. Figure 6 is presented for a better understanding of the chosen threshold value for the calculation of the flexural toughness.

3.2. Failure mode

The observed failure modes can be classified in five categories (see Figure 7) according to the geometry of the cracking pattern, the failure process and the final damage. These categories are as follow:

Mode A. Flexural failure characterised by the sudden opening of a single large crack at mid-span. This was observed for the unreinforced control specimens (N1-N4).

Mode B. Flexural failure together with the internal slip of the reinforcing mesh, which did not cause overlaying rammed earth to detach, but allowed for a large opening of a single vertical crack at mid-span. This response was observed for a case strengthened with one glass fibre mesh (G1), and the two cases with two glass fibre meshes placed at different levels (2GL1-2GL2).

Mode C. Flexural failure and detaching of the overlaying rammed earth that covered the reinforcing mesh at only one side of the specimen (asymmetric failure mode). This failure consisted of an initial opening of a vertical flexural crack at mid-span that grew during the test. Close to the maximum bending moment, discontinuous horizontal cracks that were approximately 3 cm long appeared on the lateral faces of the specimen, following the position of the reinforcing mesh and indicating the shearing process. This cracking pattern was observed on only one side of the sample. Finally, when these horizontal cracks connected, the overlaying rammed earth detached and the specimen failed. This particular failure mode was observed for most of the cases reinforced with one glass fibre mesh (G2-G4) and one of the cases that used PBO fibres (P2).

Mode D. Flexural failure and detaching of the overlaying rammed earth that covered the reinforcing mesh throughout the specimen length (symmetric failure mode). This failure was almost analogous to the previous one. The only difference was that the horizontal shearing cracks appeared at both sides of the specimen and these cracks occurred earlier, when the flexural crack was not as large as that in the previous mode. At the end, the rammed earth overlaying the reinforcing mesh was completely detached and the fibre grid slipped. This was the most repeated failure mode (9 times) and was observed for most of the carbon reinforced specimens (C1-C3) as well as for all of the basalt reinforced specimens (B1-B3), the cases with two glass fibre meshes installed at the same level (2G1-2G2) and one of the specimens reinforced with PBO (P3).

Mode E. Shear failure and the detachment of the overlaying rammed earth that covered the reinforcing mesh only at one side of the specimen. An inclined shear crack opened first, and after reaching the maximum bending moment, shearing horizontal cracks that followed the position of the reinforcing grid developed between the beginning of the large shear crack and the support of the specimen at the same side. When these horizontal cracks connected, the overlaying rammed earth detached and the sample failed. This failure mode was characteristic of the specimens reinforced with a steel grid (S1-S4), and it was also observed for a case that was reinforced with carbon fibre grid (C4) and for one of the PBO reinforced specimens (P1).

3.3. Flexural strength

The maximum applied bending moment (M_{max}) for each test is presented in the third column of Table 3. This table also includes the failure mode of each specimen (second column), the flexural toughness ($TEN_{F/10}$) in the fourth column and the average of the quantitative results for each reinforcing typology in the last two columns. These columns also include the coefficient of variation as a percentage.

It should be noted that the results from the specimen G1 were not taken into account in the calculation of the average and variation values of the glass fibre reinforced specimens because the data of the G1 test is not consistent with the comparable specimens (G2-G4).

3.4. Flexural toughness

The flexural toughness, interpreted as the area under the force vs. mid-span deflection curve (in linear scales) between the beginning of the test (origin of coordinates) and at the first point where the load reaches 10% of the maximum force in the descending branch, may be indirectly observed in the graphs shown in Figure 8. These graphs show the applied force on the vertical axis and the mid-span vertical displacement in the logarithmic scale on the horizontal axis. Using a logarithmic scale for the horizontal axis eases the visual comparison of the different tests using the same axis scale. The numerical value of the flexural toughness is shown in the fourth column of Table 3 for each specimen. The last column presents the average values for each reinforcing typology or the unreinforced cases. As previously mentioned, the data for the G1 specimen was not considered because they are not consistent with the rest of the tests.

4. Comparison and Discussion

The reinforcement system that performed better in terms of flexural strength and toughness is the one consisting of two glass fibre grids placed at different levels. The carbon fibre textile caused a minor improvement among the tested alternatives. Additionally, comparing and analysing all of the considered variables and the corresponding results may increase the understanding of the mechanical problem.

4.1. Failure mode

First, it must be noted that the unreinforced control cases (N) showed the expected failure mode (A) associated with brittle materials in flexion, namely, the opening of a single crack at the mid-span.

The failure mode of the reinforced specimens may be related to the spacing of the fibre mesh (observe Figure 7 and Table 1). It is observed that the cases with spacing between fibre tows ranging from 10 mm to 15 mm mostly show the D failure mode (flexural failure + detaching of the overlaying rammed earth that covered the reinforcing mesh throughout the specimen length). In experimental testing, it is normal for the flexural failures to show a random preference for one of the two sides of the beams/specimens. This implies that symmetric failure modes are rarely reached. Thus, the complete detachment of the rammed earth layer covering the fibre grid at both sides of the specimens in most of C (10 mm spacing), B (15 mm spacing) and 2G (12.5 mm spacing) cases seems to point at a possible lack of adherence or non-efficient mechanical bonding between the reinforcement and the rammed earth. If the rammed earth-reinforcement interface was a weak surface, the development of the observed failure mode would be justified. Moreover, the observed damage of some specimens that lost the rammed earth covering layer while they were manipulated (see Figure 4), matches the concept of having a poor connection between the fibre grids and the rammed earth on the cases that showed little spacing between fibre tows. Likewise, this particular phenomenon is not observed in the cases that had larger spacing between fibre tows (G or 2GL), which showed no detaching of the rammed earth layer (B failure mode) or the detachment of only one of the sides of the specimen (C failure mode). Introducing two fibre grids at different levels limited the deflection of specimens 2GL, which might have helped prevent the detaching of the rammed earth covering.

Finally, the shear failure mode (E) was mostly observed for the specimens that had a steel grid embedded (S) or particular cases of specimens that were reinforced with the stiffest fibres (carbon or PBO). Thus, it may be possible that the larger stiffness of these reinforcements contributed to limiting the bending deformation, leading to the shear failure of the specimen. This idea fits well with the empirical observation that the behaviour of the steel grid was more similar to a plate than to a flexible textile. In this case, the mechanical response of the grid itself as a plate influenced the structural response of the reinforced sample more than the geometrical spacing between the steel cords.

4.2. Flexural strength

First, the maximum bending moment resisted by the reinforced specimens is comparable but slightly higher than that supported by the unreinforced ones. However, the differences between the maximum applied forces (in correspondence with the applied bending moment)

of unreinforced and reinforced specimens are shown in Figure 8. This figure includes 8 graphs, the first one representing the force vs. mid-span displacement (in logarithmic scale) for the unreinforced cases (N1-N4) and the rest comparing these unreinforced specimens with the cases of each reinforcement type.

Analysing the results carefully and taking into account the qualitative evidence of the failure modes, it can be observed that all of the reinforced specimens that did not fail with the mode associated with the possible least earth-grid adherence (D failure mode) showed a greater load-bearing capacity than that of the unreinforced specimens. That is, the specimens that failed according to modes B, C and E reached greater bending moments than the unreinforced ones. The average increase of the maximum bending moment is 94% if only the mentioned cases (failure modes B, C and E) are considered.

Also, there may be a correspondence between the grid spacing and the maximum bending moment, as the cases with larger spacing reached the greatest bending moment. However, the specimens reinforced with steel grids did not follow this tendency, which might be justified by the bending stiffness of this type of reinforcement in contrast to the flexible textile fibre grids.

Finally, it is worth mentioning that the average coefficient of variation, taking into account all of the specimens (except G1), is 23.8%. This coefficient of variation, taking into account the different types of tested specimens, ranges from 4.5% for the cases that were reinforced with two glass fibre grids at the same level (2G) to 78.8% for the unreinforced cases (N). Hence, the reinforced cases show a more repeatable response. The coefficient of variation of the maximum bending moment is 16% for the reinforced specimens compared to 79% for the unreinforced cases, which is 5 times greater.

4.3. Flexural toughness

First, it was observed that all of the considered reinforcing systems contributed to increase the flexural toughness of the rammed earth specimens. This increase ranges from 260% for the carbon fibre cases (C) to 12000% for the cases reinforced with two fibre grids at different levels (2GL). Thus, although the flexural strength is not significantly improved by embedding the fibre grids, the energy required to open the cracks (measured with the flexural toughness) clearly increased when the rammed earth was internally reinforced. Thus, reinforcing new rammed earth structures with fibre grids would allow dissipating far more energy than the traditional unreinforced solution. The tail of the load-displacement curve became larger in a clear post-peak crack growth development (see Figure 8), taking into account the logarithmic scale of the horizontal axis.

Additionally, it must be noted that for the calculated values of the flexural toughness, the average coefficient of variation for all specimens (except G1) was 48.3%, ranging from 10.9% for specimens G2-G3 to 75.5% for the carbon reinforced specimens (C1-C4). In this case, the unreinforced and reinforced specimens showed similar scattering values. Thus, the flexural toughness was a variable that showed remarkable variation because it was highly influenced by the failure mode. Hence, a careful analysis of the values of the flexural toughness must be carried out and general tendencies should be obtained.

Analysing the results of the reinforced specimens, it was observed that increasing the spacing between fibre tows might lead to increasing the flexural toughness of the sample. This trend is observable (Table 3) in all cases except for those of the S series. In the case of the S series, the steel grid was far more stiff and behaved more like a plate than like a textile and therefore provided a non-comparable response. Thus, the spacing between fibre tows and the manner in which the reinforcement was connected to the earthen specimen appeared to be more significant than the quantity or type of fibres.

In addition, the normal stiffness of the reinforcement, which was calculated as the product of the Young's modulus of the fibre (E_{fib}) multiplied by the equivalent thickness (t_m), seemed to be related to the flexural toughness of the specimen. These two parameters (E_{fib} and t_m) were provided by the manufacturers and are summarised in Table 1. It was observed that the solutions with greatest stiffness (S 14.25kN/mm, P 12.42kN/mm or C 11.28kN/mm) were associated with the minor flexural toughness. That is, those specimens (G, 2G and 2GL) reinforced with less fibre and/or more deformable fibre (G 3.78kN/mm, 2G and 2GL 7.56kN/mm) obtained the greatest flexural toughness. However, the grid spacing that influenced these results and the mentioned relationship showed a tendency that requires further investigation.

Finally, it was also observed that the cases that had the greatest flexural toughness showed less scattering of this variable. This is observed through the minor coefficient of variation. Hence, increasing the energy dissipated by rammed earth elements, trough embedding fibre grid reinforcements, contributed to the homogenisation of the structural response and allowed a likely reduction of the safety factors.

4.4. Reinforcement criteria

According to the obtained results, the main criterion to reinforce a rammed earth element was assuring the connection between the reinforcement system and the earthen matrix. In the case of using textile fibre grids as reinforcement elements, the spacing between the fibre tows was the crucial parameter. The solutions with the greatest spacing were more suitable. Also, it appeared that the material of the fibres was an influencing factor. The fibres that showed a flexible response were more suitable because they helped the strain compatibility between earth matrix and fibre reinforcement.

Taking into account the obtained data, the most suitable solution (among the studied ones) was to reinforce rammed earth specimens with only one glass fibre grid, as it was associated with a large increase in the maximum bending moment and the flexural toughness. It also maintained the scattering of the response under 15%, assuring a homogeneous and repeatable behaviour.

4.5. Practical implications

The obtained results show that reinforcing new rammed earth walls would contribute to their safety when faced with out-of-plane loading conditions typically associated with wind, earthquakes or bending moments transmitted by roofs or intermediate slabs. In this line, the maximum bending moment of reinforced specimens duplicates the unreinforced ones. Hence, it can be expected that rammed earth walls reinforced with an appropriate type of grid would bear greater loads than the unreinforced ones. However, the main advantage is from the

experimentally observed flexural toughness increase of these structures, that is directly associated with a safer condition when confronted by accidental loads, including impacts, seismic actions or extraordinary wind phenomena. Reinforced rammed earth walls would be able to dissipate far more energy (more than 60 times) than unreinforced ones. Finally, the design of reinforced rammed earth walls might take into account littler safety factors to reduce the materials properties, as the scattering of the results is reduced when rammed earth walls are reinforced. From a practical viewpoint, this implies increasing the confidence of the practitioners and reducing the cost of the material.

The obtained results have the potential of practically applying this material in developed areas, where the environmental benefits and the cost reduction associated with using a local material would compensate for the expenses of introducing a high performance fibre grid (up to 80€/m^2) and the casting costs. On the other hand, this technique may also be applied in developing countries, where the increment of the costs due to the installation of the fibre grid (over 30€/m^2 for the cheapest solution among the studied ones) would be compensated by the safety increase of the resulting buildings. Moreover, using a local material (earth) would reduce the cost compared to purchasing concrete or steel in areas that are situated far from the production centres. Nevertheless, a cost/benefit study is required before any real application is carried out.

5. Conclusions

The current research achieved its main objective of providing comprehensive information about the structural response of fibre grids reinforced with rammed earth elements. The adapted testing methodology and the proposed calculation process to obtain the flexural toughness was robust and has led to useful results that were used to draw the following technical conclusions:

- The spacing between the fibre tows is the most influential variable. The connection between the earthen matrix and the reinforcement system depends on it. The structural response and the failure modes are related to the geometry of the reinforcement grid. Using grids with large spacing between tows is recommended.
- A poor connection between the reinforcing grid and the earthen matrix leads to the detachment of the rammed earth overlaying the grid because a weak surface is created. Using grids with large spacing between the tows contributes to assuring the mechanical connection with the rammed earth.
- Using high stiffness grids may contribute to limit the bending deformation that reaches shear failure and reduces the flexural toughness.
- Increasing the spacing between fibre tows may contribute to increasing the flexural toughness of the element and the maximum bending moment that it can bear.
- In the case of reinforcing with more than one grid, embedding two grids at different depths was better than reducing the spacing between fibre tows. Assuring the connection of the fibre grid was more important than providing additional depth of the reinforcement with respect to the neutral axis.

- Thus, reinforcing future rammed earth buildings may contribute to fitting the span of response and to limiting the uncertainty associated with the safety factors for project design.

In conclusion, the optimum solution to reinforce rammed earth elements is a flexible fibre grid that has large spacing between fibre tows.

6. Acknowledgements

The authors would like to acknowledge the support provided by José Antonio González Lara during the experimental campaign. This research have been carried out with the financial support of the grant 2014 PDJ 00105 from AGAUR, Generalitat de Catalunya.

7. References

[1] L. Miccoli, U. Müller, P. Fontana, Mechanical behaviour of earthen materials: A comparison between earth block masonry, rammed earth and cob, Constr. Build. Mater. 61 (2014) 327–339. doi:10.1016/j.conbuildmat.2014.03.009.

[2] H. Niroumand, M.F.M. Zain, M. Jamil, A guideline for assessing of critical parameters on Earth architecture and Earth buildings as a sustainable architecture in various countries, Renew. Sustain. Energy Rev. 28 (2013) 130–165. doi:10.1016/j.rser.2013.07.020.

[3] K. Heathcote, El comportamiento térmico de los edificios de tierra, Inf. La Construcción. 63 (2011) 117–126. doi:10.3989/ic.10.024.

[4] H. Schroeder, La transferencia de humedad y el cambio en la resistencia durante la construcción de edificios de tierra, Inf. La Construcción. 63 (2011) 107–116. doi:10.3989/ic.10.023.

[5] D. Ciancio, P. Jaquin, P. Walker, Advances on the assessment of soil suitability for rammed earth, Constr. Build. Mater. 42 (2013) 40–47. doi:10.1016/j.conbuildmat.2012.12.049.

[6] M.C. Jiménez Delgado, I.C. Guerrero, The selection of soils for unstabilised earth building: A normative review, Constr. Build. Mater. 21 (2007) 237–251. doi:10.1016/j.conbuildmat.2005.08.006.

[7] C.G. da Rocha, N.C. Consoli, A. Dalla Rosa Johann, Greening stabilized rammed earth: devising more sustainable dosages based on strength controlling equations, J. Clean. Prod. 66 (2014) 19–26. doi:10.1016/j.jclepro.2013.11.041.

[8] L. Maldonado, J. Castilla, F. Vela-Cossío, The Technic of Tapial in the Autonomous Comunity of Madrid. Use of New Materials to Consolidate rammed earth walls., Inf. La Construcción. 49 (1997) 27–37.

[9] M. Blondet, J. Vargas, N. Tarque, C. Iwaki, Construcción sismorresistente en tierra: la gran experiencia contemporánea de la Pontificia Universidad Católica del Perú, Inf. La Construcción. 63 (2011) 41–50.

doi:10.3989/ic.10.017.

[10] K. Liu, Y.A. Wang, M. Wang, Experimental and Numerical Study of Enhancing the Seismic Behavior of Rammed Earth Buildings, Adv. Mater. Res. 919-921 (2014) 925–931. doi:10.4028/www.scientific.net/AMR.919-921.925.

[11] N. Tarque, G. Camata, M. Blondet, E. Spacone, H. Varum, Numerical analyses of the in-plane response of unreinforced and reinforced adobe walls, in: 9th Int. Mason. Conf., 2014.

[12] T. Blanksvärd, B. Täljsten, Strengthening of concrete structures with cement based bonded composites, J. Nord. Concr. Res. 38 (2008) 133–154.

[13] E. Bernat, L. Gil, P. Roca, C. Escrig, Experimental and analytical study of {TRM} strengthened brickwork walls under eccentric compressive loading, Constr. Build. Mater. 44 (2013) 35–47. doi:http://dx.doi.org/10.1016/j.conbuildmat.2013.03.006.

[14] C. Escrig, L. Gil, E. Bernat-Maso, F. Puigvert, Experimental and analytical study of reinforced concrete beams shear strengthened with different types of textile-reinforced mortar, Constr. Build. Mater. 83 (2015) 248–260. doi:10.1016/j.conbuildmat.2015.03.013.

[15] E. Bernat-Maso, L. Gil, Numerical study of the performance of TRM strengthened brickwork walls against second order bending effects, in: 9th Int. Mason. Conf., Universidade do Minho. Departamento de Engenharia Civil, Guimaraes, 2014.

[16] P. Larrinaga, C. Chastre, H.C. Biscaia, J.T. San-José, Experimental and numerical modeling of basalt textile reinforced mortar behavior under uniaxial tensile stress, Mater. Des. 55 (2014) 66–74. doi:10.1016/j.matdes.2013.09.050.

[17] R. Barrionuevo, Investigación tecnológica aplicada: Domocaña, Inf. La Construcción. 63 (2011) 51–58. doi:10.3989/ic.10.025.

[18] JSCE-SF4, JSCE-SF4. Method of tests for flexural strength and flexural toughness of steel fiber reinforced concrete, JSCE Japan Soci. Civ. Eng. 3 (1984) 58–61.

[19] E. Bernat-Maso, C. Escrig, C. a. Aranha, L. Gil, Experimental assessment of Textile Reinforced Sprayed Mortar strengthening system for brickwork wallettes, Constr. Build. Mater. 50 (2014) 226–236. doi:10.1016/j.conbuildmat.2013.09.031.

List of Figures

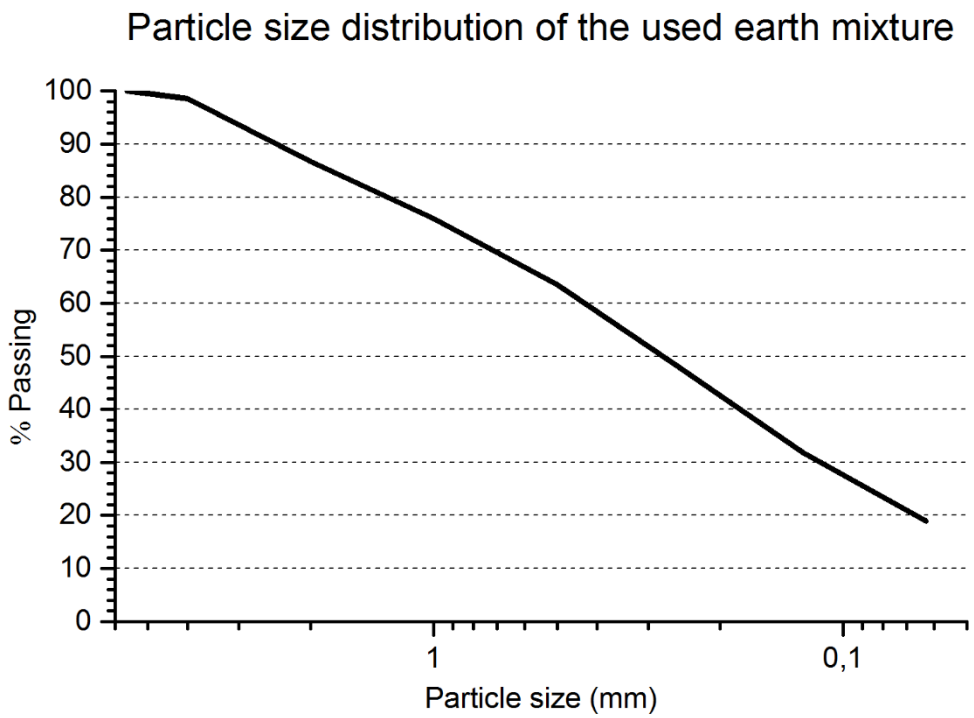

Figure 1. Nomogram of the particle size distribution of the earth components of the mixture which was used to produce the specimens.

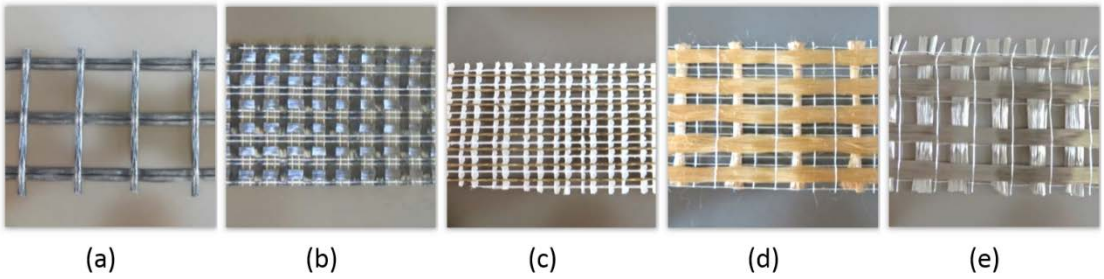

Figure 2. Strengthening grids used: (a) glass, (b) carbon, (c) steel, (d) PBO and (e) basalt.

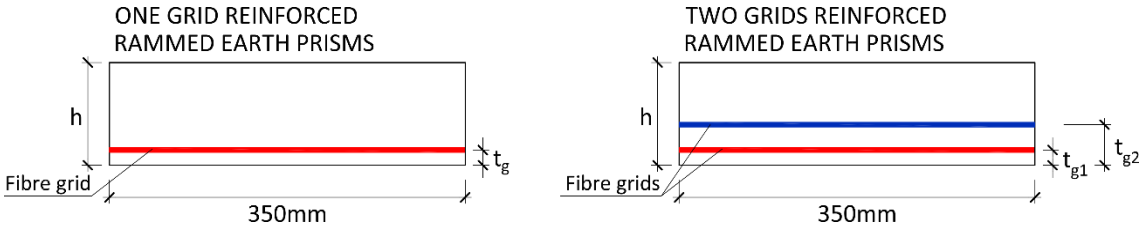

Figure 3. Dimensions of the samples and position of the fibre grids.

Figure 4. Specimen reinforced with PBO which showed the lower earth layer detached. Damaged during manipulation after curing. Not tested.

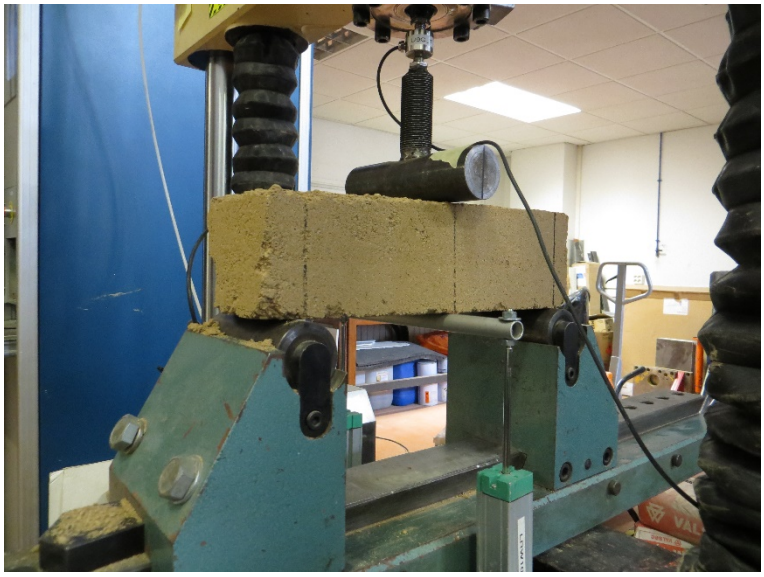

Figure 5. Test setup. Specimen on two rods (300mm of free span) and loaded at mid-span by an electromechanical press.

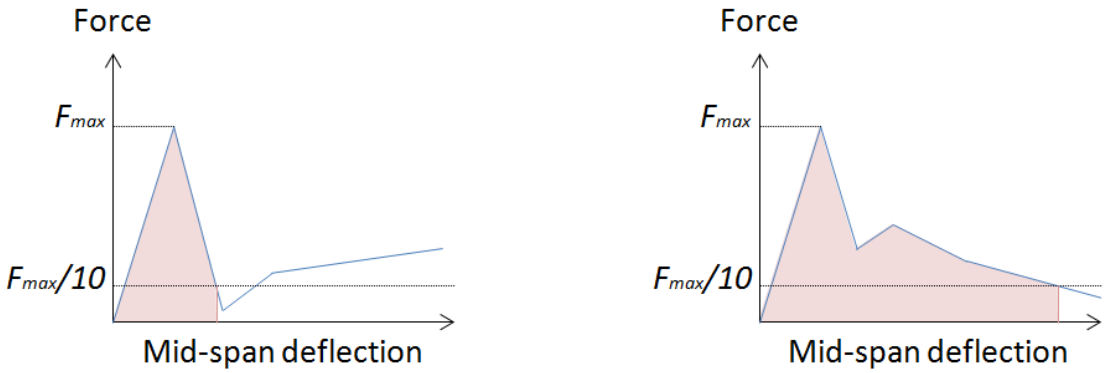

Figure 6. Threshold value for the calculation of the flexural toughness. Two hypothetical examples

	Failure mode	*Specimens*	*Picture*
A	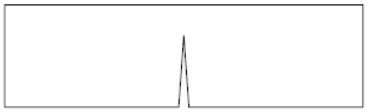	N1-4	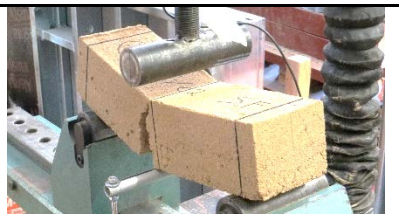
B	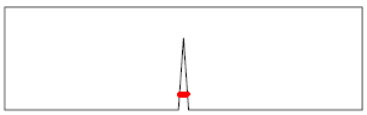	G1; 2GL1-2	
C	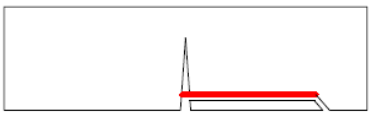	G2-4; P2	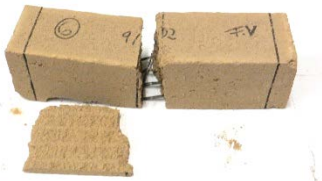
D	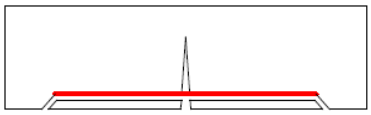	C1-3; P3; B1-3; 2G1-2	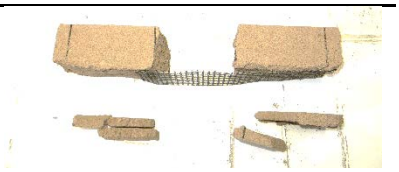
E	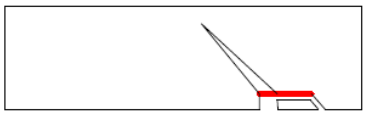	C4; S1-4; P1	

Figure 7. Failure mode of the testes specimens

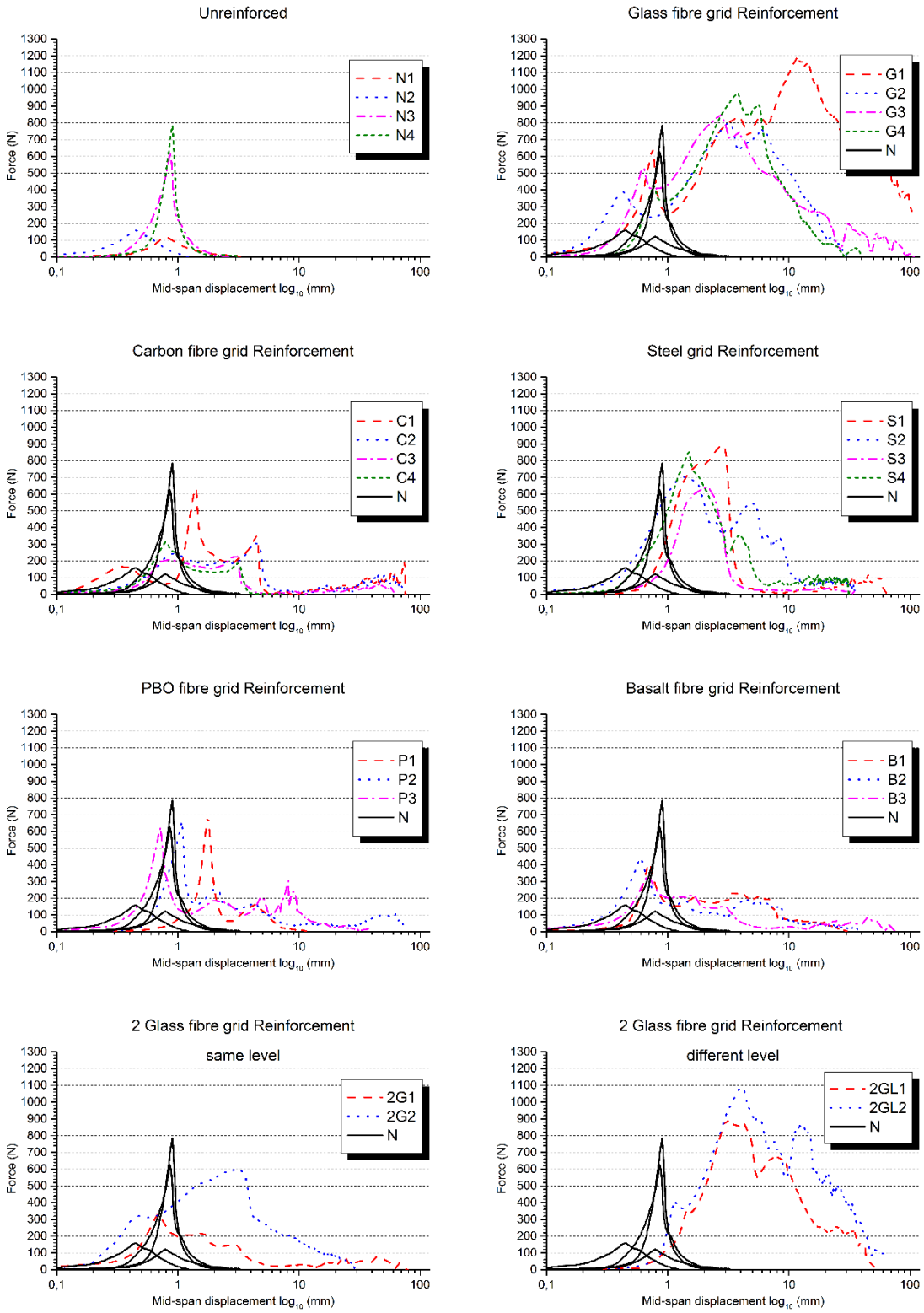

Figure 8. Structural response of the samples. Comparison with cases without fibres.

List of tables

Fibre type			***Glass (G)***	***Carbon (C)***	***Steel (S)***	***PBO (P)***	***Basalt (B)***
Fibre	Orientation*		Bi	Bi	Uni	Uni	Bi
	Ultimate tensile strength	f_{fib} [MPa]	2610	4320	3070	5800	2990
	Young's modulus	E_{fib} [GPa]	90	240	190	270	95
	Ultimate strain	ε_{fib} [%]	2.90	1.80	1.60	2.15	3.15
Grid	Weight	w [g/m^2]	225	168	600	88	200
	Tow width	b_m [mm]	3	4	0.8	5	5
	Distance between tows	s_m [mm]	25	10	5	10	15
	Equivalent thickness	t_m [mm]	0.042	0.047	0.075	0.046	0.053
	Colour		Black	Black	Golden	Golden	Grey
	Texture†		C	U	C	U	U

* Bi: Bidirectional orientation / Uni: Unidirectional orientation

† C: Coated / U: Uncoated

Table 1. Properties of the fibres and grids used to reinforce the rammed earth samples

Specimen	***Reinforcing grid***	***Width, b (mm)***	***Height, h (mm)***	***Position of fibre grid, t_g (mm)***
N1	No grid	102	98	---
N2	No grid	102	95	---
N3	No grid	102	86	---
N4	No grid	103	84	---
G1	Glass fibre	101	92	13
G2	Glass fibre	102	94	13
G3	Glass fibre	103	92	19
G4	Glass fibre	102	87	18
C1	Carbon fibre	102	100	19
C2	Carbon fibre	102	96	19
C3	Carbon fibre	102	91	16
C4	Carbon fibre	102	98	23
S1	Steel	101	97	18
S2	Steel	102	98	23
S3	Steel	102	92	26
S4	Steel	102	98	28
P1	PBO fibre	100	90	18
P2	PBO fibre	98	94	25
P3	PBO fibre	102	94	30
B1	Basalt fibre	101	93	17
B2	Basalt fibre	103	98	12
B3	Basalt fibre	100	96	18
2G1	2 glass fibre grids same level	101	96	28
2G2	2 glass fibre grids same level	103	93	23
2GL1	2 glass fibre grids diff. levels	103	95	25/45
2GL2	2 glass fibre grids diff. levels	103	98	26/45

Table 2. Geometrical properties and material components of the tested specimens

Specimen	*Failure mode*[a]	M_{max} *(Nm)*	$TEN_{F/10}$ *(mJ)*	$\overline{M_{max}}$ $(Nm)^c$	$\overline{TEN_{F/10}}$ *(mJ)*[c]
N1	A	9.1	89	31.7 (78.8)	152 (56.4)
N2	A	11.9	69		
N3	A	46.8	237		
N4	A	58.8	215		
G1[b]	B	89.6	63117	65.7 (10.5)	8840 (10.9)
G2	C	60.0	9652		
G3	C	63.8	9089		
G4	C	73.4	7778		
C1	D	47.6	62	28.1 (47.3)	551 (75.5)
C2	D	22.9	1079		
C3	D	18.1	552		
C4	E	23.6	512		
S1	E	67.1	1914	57.9 (15.7)	2324 (56.3)
S2	E	52.7	4199		
S3	E	47.9	1154		
S4	E	64.0	2028		
P1	E	51.6	393	49.3 (5.0)	1093 (67.9)
P2	C	49.6	1015		
P3	D	46.7	1871		
B1	D	30.8	2225	29.6 (14.7)	1484 (54.2)
B2	D	33.3	1599		
B3	D	24.8	629		
2G1	D	42.1	2945	43.5 (4.5)	3759 (30.6)
2G2	D	44.9	4572		
2GL1	B	67.2	14094	74.5 (13.8)	18645 (34.5)
2GL2	B	81.8	23197		

[a] According with Figure 7.
[b] Discarded data in the calculation of the average values.
[c] Coefficient of variation in brackets (%).

Table 3. Results of the experimental campaign.